Author Manuscript

Author Manuscript

Author Manuscript

Author Manuscript

HHS Public Access

Author manuscript

J Proteome Res. Author manuscript; available in PMC 2021 July 05.

Published in final edited form as:

J Proteome Res. 2021 April 02; 20(4): 1918–1927. doi:10.1021/acs.jproteome.0c00938.

Improved SILAC quantification with data independent acquisition to investigate bortezomib-induced protein degradation

Lindsay K Pino[1], **Josue Baeza**[1], **Richard Lauman**[1], **Birgit Schilling**[2], **Benjamin A Garcia**[1,*]

[1]Department of Biochemistry and Biophysics, University of Pennsylvania, Philadelphia, PA, U.S.A.

[2]Buck Institute for Research on Aging, Novato, CA, U.S.A.

Abstract

Stable isotope labeling by amino acids in cell culture (SILAC) coupled to data-dependent acquisition (DDA) is a common approach to quantitative proteomics with the desirable benefit of reducing batch effects during sample processing and data acquisition. More recently, using data-independent acquisition (DIA/SWATH) to systematically measure peptides has gained popularity for its comprehensiveness, reproducibility, and accuracy of quantification. The complementary advantages of these two techniques logically suggests combining them. Here, we develop a SILAC-DIA-MS workflow using free, open-source software. We determine empirically that using DIA achieves similar peptide detection numbers as DDA and that DIA improves the quantitative accuracy and precision of SILAC by an order of magnitude. Finally, we apply SILAC-DIA-MS to determine protein turnover rates of cells treated with bortezomib, a 26S proteasome inhibitor FDA-approved for multiple myeloma and mantle cell lymphoma. We observe that SILAC-DIA produces more sensitive protein turnover models. Of the proteins determined differentially degraded by both acquisition methods, we find known ubiquitin-proteasome degrands such as HNRNPK, EIF3A, and IF4A1/EIF4A-1, and a slower turnover for CATD, a protein implicated in invasive breast cancer. With improved quantification from DIA, we anticipate this workflow making SILAC-based experiments like protein turnover more sensitive.

Graphical Abstract

*corresponding author, bgarci@pennmedicine.upenn.edu.

Author Manuscript Author Manuscript Author Manuscript Author Manuscript

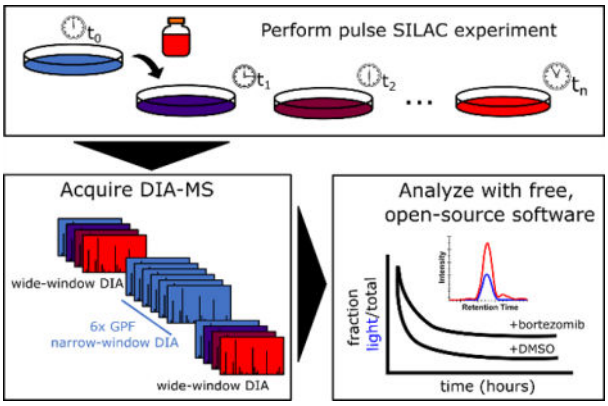

Keywords

protein turnover; pulse SILAC; protein degradation; data independent acquisition; quantitative proteomics

INTRODUCTION

There are generally two approaches to quantitative bottom-up proteomics: those involving isotopic labeling and those label-free[1,2]. The former includes strategies such as isobaric labeling using chemical tags and metabolic labeling, such as stable isotope labeling by amino acids in cell culture (SILAC), in which proteins are metabolically labeled in vivo with heavy isotope-containing amino acids, pooled together prior to sample preparation[3]. Quantitative SILAC workflows have been typically analyzed by data dependent acquisition (DDA) using MS1 precursor ion abundances for quantification. Here we present a novel strategy using data independent acquisition (DIA) and MS2 chromatogram quantification, where SILAC samples are prepared individually and acquired by DIA separately[4]. Then, the two individual MS2 chromatograms are compared to determine differential abundance. An advantage of using metabolic isotopic labeling is the ability to multiplex the samples, and the mass spectrometry acquisition of pooled samples reduces technical variation. However, a clear advantage of DIA is that the MS2-level quantification is typically more reproducible and accurate[5].

Interest in multiplexing DIA experiments by isotopic labeling has led to the exploration of neutron-encoded (NeuCode) SILAC (NeuCoDIA)[6] and mass defect based four-plex data-independent acquisition (MdFDIA)[7]. Isobaric tagging (e.g. TMT, iTRAQ) is not possible in DIA acquisition modes because reporter ions from multiple precursors become convoluted and cannot be linked back to the precursor of origin[8]. While precursor mass-shifting multiplexing approaches seem promising, there is still a need for fundamental benchmarking to explicitly compare SILAC-DDA versus SILAC-DIA.

Benchmarking is especially necessary because, in theory, SILAC increases the complexity of a sample by the number of labels used. A conventional two-plex SILAC experiment with a light and a heavy proteome combined together is then twice as complex as the equivalent label-free experiment. Due to this increased complexity, there is an expectation that

Author Manuscript Author Manuscript Author Manuscript Author Manuscript

conventional SILAC-DIA/SWATH approaches should underperform conventional SILAC-DDA workflows[9]. While comparisons of SILAC-DDA versus DIA-MShave been explored[10] and SILAC labeling is supported in DIA analysis softwares such as Spectronaut[11], there are few explicit comparisons of SILAC-DDA versus SILAC-DIA. However, it has been shown that SILAC increases the reproducibility DIA quantifications[12], and there are experimental designs that require the incorporation of metabolic labels like SILAC including Isotopic Differentiation of Interactions as Random or Targeted (I-DIRT) for protein-protein interactions[13] and pulse SILAC for protein turnover.

Pulse SILAC (pSILAC) is the predominant method to study protein turnover at the proteome scale, enabling the discrimination of preexisting and newly synthesized proteins[14–16]. Using pSILAC, the cell's translational machinery is used to incorporate stable isotope labeled amino acids present in the cell media, thereby marking newly synthesized proteins. Over time, as proteins are synthesized and degraded (also called protein turnover), the levels of the newly synthesized proteins increase while the preexisting proteins decline allowing protein half-lives to be determined. This approach has been used to explore proteostasis in a number of biological systems, including differentiation[17], cancer homeostasis[18], drug treatment response[19–21], and the accumulation of "old" proteins in aging[22].

Given the broad range of biological systems that benefit from pulse SILAC turnover studies, and considering the quantitative benefits of DIA-MS approaches, we sought to accelerate turnover studies by validating the hyphenation of these two technologies and establishing a freely available analysis workflow.

EXPERIMENTAL SECTION

Cell culture medium.

Cell culture medium was prepared from Dulbecco's Modified Eagle Media (DMEM) (Thermo Fisher) supplemented with 10% dialyzed fetal bovine serum (FBS) (Atlanta Biologicals) and 1% penicillin & streptomycin (Gibco, Life Technologies Corporation, Grand Island, NY, USA). For SILAC experiments, DMEM for SILAC (Thermo Fisher) which is deficient in arginine, and lysine is supplemented with 10% dialyzed fetal bovine serum (dFBS) and 1% Pen/Strep. Light SILAC media is supplemented with L-arginine HCl (84 mg/L), L-lysine HCl (146 mg/L) and L-proline (1000 mg/L). Heavy SILAC media is supplemented with with L-arginine-$^{13}C_6$, $^{15}N_4$ HCl (88.2 mg/L), L-lysine-$^{13}C_6$, $^{15}N_2$ HCl (190.59 mg/L) and L-proline (1000 mg/L) (Cambridge Isotope Laboratories, Andover, MA). Media components were mixed and sterile-filtered through a 0.22 um PES membrane filter (Millipore).

HeLa SILAC labeling for benchmarks.

HeLa cells were cultured in heavy- and light-SILAC culture media continuously for 11 days. The labeled media were removed and the cells were quickly washed twice with sterile PBS at room temperature, scraped off the dishes, pelleted by centrifugation, snap-frozen in liquid nitrogen, and stored at −80 °C.

Author Manuscript Author Manuscript Author Manuscript Author Manuscript

Bortezomib pulse-SILAC labeling.

Primary human foreskin fibroblasts (HFF) were cultured in DMEM, 10% FBS, 1% Pen/Strep. Prior to pulse-SILAC labeling, HFF cells were conditioned to the SILAC media formulation over four cell passages. With each passage, HFF cells were cultured with an increasing amount of SILAC media which increased in increments of 25%. Passage 1: 75% DMEM, 25% SILAC DMEM; passage 2: 50% DMEM, 50% SILAC DMEM; passage 3: 25% DMEM, 75% SILAC DMEM; passage 4: 100% SILAC DMEM. After culture in light media, HFF were supplemented with DMSO or 1000 pM Bortezomib and concurrently the media was switched to SILAC DMEM. Cells were harvested together after 0, 2, 4, 8, 10, 24, 48, 72, 168, and 500 hours of labeling, washed in PBS, and stored in −80 °C until further analysis.

Human cell line protein preparation.

Cell pellets were resuspended in lysis buffer (8M urea, 75mM NaCl, 50mM Tris pH 8, 1mM EDTA pH 8) and sonicated 3x for 30s, resting on ice in between. Protein concentration was estimated by BCA (Pierce BCA Protein Assay Kit, Thermo Scientific, Rockford, IL, USA). Denatured proteins were reduced with 5 mM DTT, alkylated with 15 mM IAA, and digested overnight with 1:50 trypsin (Promega). Peptides were desalted using an MCX protocol (Oasis MCX cartridge 1cc/30 mg LP, Waters Corporation) and dried down by speed-vac. To generate light/heavy mixtures, light and heavy HeLa peptides were reconstituted to 1 ug/ul and the concentrations adjusted to 1:1 using TIC. Peptides were used to construct a calibration curve spanning three orders of magnitude via five serial dilutions (Supplementary Table 1).

E. coli protein preparation.

E. coli pellets were available that were either previously labeled with stable isotope labeled lysine residue ($^{13}C_6$-$^{15}N_2$-Lys) (no heavy arginine was used in these samples) growing them in heavy SILAC media from Cambridge Isotopes (heavy samples), or they were grown in regular media (light samples). We then processed isolated frozen bacterial pellets. Cell pellets of the heavy and light *E. coli* strains were suspended in 6 mL of PBS and centrifuged at 4°C, 15,000 g for 20 min. The firm cell pellet was collected and re-suspended and denatured in a final solution of 6 M urea, 100 mM Tris, 75 mM NaCl.

Protein lysates containing 1 mg of protein were reduced with 20 mM DTT in 100 mM Tris (37°C for 1 h), and subsequently alkylated with 40 mM iodoacetamide in 100 mM Tris (30 min at RT in the dark) (Sigma Aldrich, St. Louis, MO). Samples were diluted 10-fold with 100 mM Tris (pH 8.0) and incubated overnight at 37°C with sequencing grade trypsin (Promega, Madison, WI) added at a 1:50 enzyme:substrate ratio (wt/wt). Subsequently, samples were acidified with formic acid and desalted using HLB Oasis SPE cartridges (Waters, Milford, MA)[23]. Proteolytic peptides were eluted, concentrated to near dryness by vacuum centrifugation, and re-suspended chromatographic (aqueous) buffer A. To generate light/heavy mixtures, light and heavy *E. coli* peptides were diluted spanning 400x range (Supplementary Table 2).

Author Manuscript Author Manuscript Author Manuscript Author Manuscript

Orbitrap liquid chromatography-mass spectrometry for human cell line samples.

Peptides were analyzed with a Thermo Dionex UPLC coupled with a Thermo Q-Exactive HFX tandem mass spectrometer. We used an in-house pulled column created from 75 μm inner diameter fused silica capillary packed with 2.4 μm ReproSil-Pur C18 beads (Dr. Maisch) to 30 cm. Solvent A was 0.1% formic acid in water, while solvent B was 0.1% formic acid in 80% acetonitrile. For each injection, we loaded approximately 1 μg peptides and separated them using a 90-minute gradient from 5 to 35% B, followed by a 50 min washing gradient.

For data dependent acquisition (DDA) analysis, a Top20 method was used (default charge state 3, minimum AGC target 5e4, charge exclusion 1 and >8, and dynamic exclusion 15s) with full MS (resolution 120,000; AGC 1e6, maximum IT 40 ms) and data dependent-MS2 (resolution 15,000; AGC 2e5, max IT 40 ms, isolation window 2.0 m/z, NCE 27)).

For data independent acquisition (DIA) analysis of the dilution series and bortezomib experiments, we performed chromatogram library experiments as described in Searle *et al*[24]. Briefly, we acquired 6 chromatogram library acquisitions with 4 m/z DIA spectra (4 m/z precursor isolation windows at 30,000 resolution, AGC target 1e6, maximum inject time 60 ms, 27 NCE) using a staggered[25] (also referred to as overlapping) window pattern from narrow mass ranges using window placements optimized by Skyline (i.e., 398.43–502.48, 498.48–602.52, 598.52–702.57, 698.57–802.61, 798.61–902.66, and 898.6–1002.70 m/z). We acquired corresponding precursor spectra matching the range (i.e., 390–510, 490–610, 590–710, 690–810, 790–910, and 890–1010 m/z) using an AGC target of 1e6 and a maximum inject time of 60 ms were interspersed every 25 MS/MS spectra.

For all single-injection acquisitions, the Thermo Q-Exactive HFX was configured to acquire either 75 × 8 m/z (covering 400–1,000 m/z) precursor isolation window DIA spectra (15,000 resolution, AGC target 1e6, maximum inject time 20 ms, 27 NCE) using an optimized staggered window pattern. Precursor spectra (target range ± 15 m/z at 60,000 resolution, AGC target 1e6, maximum inject time 60 ms) were interspersed every 75 MS/MS spectra. Isolation window schemes for the pulse SILAC experiments have been previously described[26] and the additional windowing schemes benchmarked in this work including method settings are detailed in Supplemental Table 3.

QqTOF Liquid-Chromatography-Mass Spectrometry Acquisitions of E. coli samples.

Briefly, samples were analyzed by reverse-phase HPLC-ESI-MS/MS using an Eksigent Ultra Plus nano-LC 2D HPLC system (Dublin, CA) with a cHiPLC system (Eksigent) which was directly connected to a quadrupole time-of-flight (QqTOF) TripleTOF 6600 mass spectrometer (SCIEX, Concord, CAN). After injection, peptide mixtures were loaded onto a C18 pre-column chip (200 μm × 0.4 mm ChromXP C18-CL chip, 3 μm, 120 Å, SCIEX) and washed at 2 μl/min for 10 min with the loading solvent (H2O/0.1% formic acid) for desalting. Subsequently, peptides were transferred to the 75 μm × 15 cm ChromXP C18-CL chip, 3 μm, 120 Å, (SCIEX), and eluted at a flow rate of 300 nL/min with a 3 h gradient using aqueous and acetonitrile solvent buffers (Burdick & Jackson, Muskegon, MI).

Author Manuscript Author Manuscript Author Manuscript Author Manuscript

For quantification, all *E. coli* peptide samples were analyzed by data-independent acquisition (DIA), using 64 variable-width isolation windows[5,27]. The variable window width is adjusted according to the complexity of the typical MS1 ion current observed within a certain m/z range using a DIA 'variable window method' algorithm (more narrow windows were chosen in 'busy' m/z ranges, wide windows in m/z ranges with few eluting precursor ions). DIA acquisitions produce complex MS/MS spectra, which are a composite of all the analytes within each selected Q1 m/z window. The DIA cycle time of 3.2 sec included a 250 msec precursor ion scan followed by 45 msec accumulation time for each of the 64 variable SWATH segments.

DIA data analysis.

Mass spectrometry data files were demultiplexed and converted to MZML using MSConvert (version 3.0.18)[28]. For single-shot, "direct" DIA experiments, MZML files were searched against the human reference proteome (20350 entries, accessed 2019/10/16) using Walnut (version 0.9.5). For pulseSILAC experiments (dilution series, bortezomib), the processing workflow is depicted schematically in Figure 1. First, narrow window GPF-DIA-MS data was searched against a predicted spectral library to generate a chromatogram library[29,30]. The chromatogram library was used to search the endogenous, light SILAC peptides in each of the curve points using EncyclopeDIA (version 0.9.0). The resulting elib file was imported into Skyline as a library, the detected light peptides used to populate the Target List, and heavy SILAC pairs were associated with each detected peptide sequence. Only y-ions were included for quantification, ensuring that each fragment ion contains the light/heavy amino acid. Demultiplexed MZML data files were then imported into Skyline to extract light and heavy SILAC chromatograms. For a full tutorial on analyzing SILAC-DIA with this method, see Supplementary Note 1.

DDA data analysis.

RAW files were converted to MZML using MSConvert (version 3.0.18). MetaMorpheus (version 0.0.310)[31] was run with the following parameters: trypsin, 2 max missed cleavages, minimum peptide length 7; fixed carbamidomethyl on C and U, variable oxidation on M; precursor mass tolerance 5 ppm, product mass tolerance 20 ppm; HCD fragmentation. SILAC/SILAM quantification (multiplex) was selected using R(+10.008) & K(+8.014) labels, with "quantify unlabeled peptides/proteins" enabled.

Data availability.

The RAW files, converted MZML files, Metamorpheus output files, Encyclopedia elib files, and Skyline documents have been deposited in ProteomeXChange Consortium[32] via the Panorama[33] partner repository with the identifiers PXD022659 (ProteomeXchange) and https://panoramaweb.org/silac-dia.url (Panorama).

Statistical determination of turnover rate.

Ratios were calculated each for each replicate. Specifically, for each replicate, we use the Skyline-reported Total Area Fragment value (MS2, y-ions only) for Light and Heavy isotopes to calculate the ratio. For the labeling methods in this work, it was crucial to only

Author Manuscript Author Manuscript Author Manuscript Author Manuscript

use y-ions because only that fragmentation series includes the N-terminal SILAC label, ensuring that the fragment m/z is specific to the light or heavy precursor. Protein turnover was determined by fitting the peptide-level data for each protein to an exponential function by nonlinear least squares ("nls" function in the R package "stats", version 4.0.2) as described by Welle *et al*[34] to obtain the first-order degradation rate constant (k_{deg}) for each protein. Specifically,

$$ratio = \frac{light}{(heavy + light)} = e^{-k_{deg} * time}$$

in which *time* is the duration of culture in the heavy media. Each protein turnover model was allowed to run for a maximum of 1000 iterations with all peptide-level data reported for each protein group, else k_{deg} was reported as missing. The result is a k_{deg} value for each peptide with light and heavy quantifications in each condition (here, DMSO and bortezomib treatments).

The k_{deg} is then converted to the time to protein degradation ($halflife_{hours}$), as estimated by each peptide and in each condition, by

$$halflife_{hours} = \frac{log(2)}{k_{deg}}$$

The half-lives (above) were then fit to a linear model to determine significantly differential half-lives under bortezomib treatment.

The code is available on Github (https://github.com/lindsaypino/silac-dia.git).

RESULTS AND DISCUSSION

Despite interest in multiplexing DIA, such as by SILAC-DIA, there is concern about splitting the isotopic distributions of paired precursor species. To illustrate the theory, we simulated isotopic envelopes from the human proteome (Supplemental Figure 1). In an ideal scenario, the heavy isotopic envelope will still fall entirely within the DIA isolation window adjacent to its endogenous paired species. However, there are also undesirable scenarios where one of the SILAC pairs has an isotopic envelope split across two adjacent DIA windows. The concern then, which has been raised by others including Ludwig *et al*[9], is whether these split isotopic envelopes will affect DIA peptide detections or quantification.

We first approached addressing this theoretical concern by assessing the question of detection in SILAC-DDA vs SILAC-DIA experiments. To do so, we constructed three benchmark samples: a 100% SILAC light proteome, a 100% SILAC heavy proteome, and a 1:1 equimolar mix of SILAC light and heavy. We acquired these three benchmark samples in triplicate by both DDA and DIA, then analyzed the samples using MetaMorpheus and Walnut, respectively. We found that the number of detections in the DDA and the DIA samples is comparable (Figure 2A). The number of detections made by DDA in the 50/50% sample is much lower than in either 100% sample, likely owing to the increased complexity in the 50/50% sample. By doubling the complexity of the sample, roughly 50% of the

Author Manuscript Author Manuscript Author Manuscript Author Manuscript

precursor ions presented to a DDA method will be the redundant SILAC pairs, pointing to a potential pitfall of using DDA for SILAC applications. With this in mind, in single-shot samples, it does not appear that isotopic envelope splitting negatively impacts the number of detections by DIA.

We then tested two DIA windowing schemes to determine the effect of isolation window width and staggering on peptide detections. We hypothesized that, if isotopic envelope splitting across windows affected peptide detection, then fixed windows would improve detections. However, we find that staggered windows achieve slightly better detections than fixed windows (Figure 2B), further supporting that isotopic envelope splitting across DIA isolation windows does not greatly affect peptide detections in empirical data.

Next, we determined whether SILAC would affect quantitative accuracy. For these experiments, we used similar benchmark samples as above (e.g. a 100% light- and a 100% heavy-labeled HeLa proteome), but rather than combining them 1:1, we made serial dilutions spanning several orders of magnitude, resulting in a 70% heavy sample down to a 0.1% heavy. Because the expected ratio of light to heavy is known, we can compare the measured ratio to assess quantitative accuracy[35]. In the DDA dataset, as the sample ratio gets more extreme, there are less proteins detected, due to increasing missingness in the data which makes ratio calculations impossible (Figure 3A). Additionally, as the ratios get more extreme, the measured ratios deviate farther from the expected value. This is especially apparent when comparing the measured ratios for the 70%, 50%, 30%, and 10% ratio samples, where the ratio is reasonably measured, to the 1% ratio sample, which is greatly overestimated by the observed measurements. However, when we measure the same samples by DIA, we have far more measured ratios, due to less missing values (Figure 3C). The number of detected peptides is higher, and while the amount of measured ratios does decrease as the sample ratios get more extreme, there are many more measurements by DIA than by DDA.

Further, we see an extended dynamic range by DIA. Although we measure the same highest-abundance peptides, there are many more points extending into the less abundant peptides. Despite lower overall measurements in the most extreme ratio, DIA gained an order of magnitude more sensitivity in peptide ratios than DDA (Figure 3B, 3D). Therefore, it does not appear that isotopic envelope splitting is negatively affecting the SILAC quantifications, at least not as negatively as DDA baseline measurements.

We also measured a similar sample set using *E. coli* on a TripleTOF 6600 system, in which a range of light and heavy *E. coli* ratios (20:1 through 1:20) were assessed for quantitative accuracy comparing MS1 measurements (top ranked precursor) and MS2 measurements (EncyclopeDIA-refined fragment ions) of the same DIA files (Supplemental Figure 2). Over this 400x range, the ratios measured by MS2-based SILAC-DIA more closely reproduced the expected ratios especially at the extremes. We further investigated the differences in quantification by comparing the coefficient of variation (CV) of the technical replicates when measured by MS1 or MS2, and we found that overall, MS2-level estimates are more reproducible than MS1-level. At the largest light/total fraction (20:1) the CVs are nearly identical (MS1 median 12%, MS2 median 14%) while at the smallest fractional ratio (1:20)

Author Manuscript Author Manuscript Author Manuscript Author Manuscript

MS2-level quantification is more reproducible (MS1 median 60%, MS2 median 22.5%). Therefore, not only is pSILAC-DIA MS2-level quantification more accurate in capturing known ratios, it is also more reproducible in those measurements as well. These experiments demonstrate that SILAC-DIA works for QTOF systems as well as the Orbitrap systems used elsewhere in this work.

To explore whether these qualitative and quantitative benefits translate to biological experiments, we performed a pulse SILAC experiment to determine changes in protein turnover associated with inhibiting the proteasome by bortezomib treatment. Bortezomib is the first FDA-approved proteasome inhibitor for treating cancer (multiple myeloma), and therefore we expect that proteins that are degraded by the ubiquitin-proteasome pathway will have decreased turnover rate (increased half-life) in this condition. We dosed cells with either DMSO or bortezomib simultaneously at the time of the SILAC heavy media switch. Using the fractional abundance from each of the ten time points, we fit a nonlinear model to each of the proteins (Figure 4A, 4B). We observed that the distribution of protein turnover models based on the two underlying datasets are overall similar, but that models of longer half-lives (decreased turnover) are more disparate compared between DDA and DIA (Supplemental Figure 4). This is in part because, with DIA, ratios roughly an order of magnitude more sensitive can be measured by DIA than by DDA. Additionally, with the DDA data, smaller fractions were more prone to missing values, which is again reflected in these turnover models because there is not enough data at the lower fractions to fit the model. Finally, we note the difference in quantitative dynamic range between the DDA and DIA model distributions, which is also observed in the quantitative benchmarking, recurring again in this application as increased dynamic range in turnover models.

We compared the differentially degraded proteins as determined using the DDA quantification or the DIA quantification (Figure 4C, 4D) (Supplemental Data 1). A limitation in the workflow approach presented here for pulseSILAC-DIA data processing is that it does not consider any heavy peptides that are not originally present in the light channel, so if there’s some new protein that is present in heavy but not in light, then that protein would not be measured by this method (false negative). Additionally, we have found that a challenge common to all turnover proteomics is the difficulty in calculating protein half-lives and performing differential testing. Here, we perform stringent filtering at the peptide level, only using peptides measured in at least eight of the ten time points, to fit the half-life model. Further, we perform differential testing for proteins with at least three peptides, in order to calculate a mean and variance for each protein half-life, which has excluded many proteins especially from the DIA data analysis. In the future, developing more robust and easy-to-use open-source software for calculating half-lives and performing differential testing for turnover experiments would greatly advance the proof-of-concepts shown here.

Although the DDA data tested less proteins for differential degradation, it produced more statistically significant proteins. Specifically, of the 622 proteins tested for differential degradation in the DDA data, 52 were determined statistically significant (q-value < 0.05); of the 1373 proteins tested in the DIA data, 34 were determined statistically significant. The DDA-based significant proteins were estimated from an average of 20 peptides per protein;

Author Manuscript Author Manuscript Author Manuscript Author Manuscript

the DIA-based significant proteins were estimated from an average of 13 peptides per protein. Of the 52 significant proteins by DDA, 3 proteins were detected in the DIA dataset but did not have sufficient peptides to estimate a variance (<3 peptides detected per protein); likewise, of the 34 significant proteins by DIA, 5 were detected by DDA but with only two peptides. It follows that a more robust differential test that isn't dependent on a minimum of three peptides to estimate variance could improve the agreement between these two methods. At the peptide level, there is a correlation between the half-life calculated from the DDA and DIA data (Supplemental Figure 5), suggesting that disagreement between the two datasets arises in part from rolling peptide values up to protein level. The larger number of significantly differential proteins by DDA is possibly due to the lower number of total tested proteins. Because over twice as many proteins were statistically tested with the DIA dataset, multiple hypothesis correction impacts that dataset more than the DDA dataset. We also examined the reproducibility of half-life estimation using DDA- and DIA-based measurements using two technical replicates each of the SILAC light/heavy ratio samples in Figure 3 (Supplemental Figure 7). A reproducible half-life estimate should produce the same value in both replicates (y=x) in these plots. We find that the DIA data provides more reproducible half-life values, with a regression closer to the expected y=x equation which would have a slope of 1 and an intercept of 0 (DIA slope = 0.6746, intercept = 0.6354) compared to the DDA half-life reproducibility (DDA slope = 0.6025, intercept = 1.323). Not only is the DIA half-life reproducibility closer to the expected y=x correlation, the DIA data is also closer to its fitted regression line (R^2 = 0.655) compared to the DDA regression (R^2 = 0.472). This demonstrates that the half-life values modeled from DIA data are more reproducible than the half-life values modeled from DDA data, and may contribute to false positives when performing differential turnover testing.

The two datasets both revealed 12 proteins (Table 1) with similar, significant changes to protein half-life. By inhibiting the proteasome with bortezomib, we expect that more proteins should be present for a longer time, because they are not degraded by the proteasome. We observe that most of these proteins have positive log2 FC, indicating that the protein is present for a longer time (is not degraded) under bortezomib treatment as expected. Of note, the ubiquitin-proteasome pathway is known to degrade HNRNPK[36] and inhibition of the proteasome shows increased levels of HNRNPK, supporting our results. Additionally, the 20S proteasome has been shown to degrade EIF3A and IF4A1/EIF4A-1[37], which we also observe here in the form of decreased degradation under proteasome inhibition. We also note that three proteins appear to be degraded faster (or synthesized more) under bortezomib treatment. Two of these three proteins, DHB4 and CATD, are also known to have cleaved forms, which may not be detected by the approach performed here as it only considers the protein level. Increased half-life of these proteins may indicate that, after time zero and treatment with bortezomib, the protein can no longer be cleaved into its products. More elegant models, either for protein quantification or for differential turnover at the peptide level, would potentially be useful for such systems as bortezomib treatment, which may affect not only global protein abundances but also cleavage isoforms. The decrease in Cathepsin D (CATD) degradation half-life measured here could also be explained by an increased synthesis rate, as cathepsin D is an aspartyl protease and could be upregulated to counter the cell's inability to degrade proteins via the bortezomib-inhibited

Author Manuscript Author Manuscript Author Manuscript Author Manuscript

ubiquitin-proteasome pathway. Increases in CATD due to either increased transcription rates or alternative processing of the pro-CATD gene product have been linked to breast cancer metastasis[38].

CONCLUSIONS

The experiments described here validate the combination of SILAC together with DIA, demonstrating that the theoretical concern for isotopic envelope splitting detrimentally affecting peptide detection and quantification is not observed in empirical data. Using benchmarking data sets, we show that conventional DIA methods can be used for SILAC samples and that narrower DIA isolation window methods outperform wider window schemes in peptide detection; but multiplex SILAC-DIA does not detect as many peptides as multiplex SILAC-DDA. Less peptides are detected in the 100% light and 100% heavy samples when the search space contains both light and heavy precursors likely due to the search algorithm (Walnut) having difficulty with handling the doubled search space. However, that limitation is overcome in the 50/50% sample because then the DDA approach is limited in that half the topX DDA precursor peaks are redundant isotope pairs.

SILAC-DIA truly outperforms not in peptide detections but rather in peptide quantification, achieving an order of magnitude more depth in quantitative accuracy compared to conventional SILAC-DDA. We also demonstrate that SILAC-DIA quantification matches expected ratios not only for Orbitrap systems using fixed and staggered windows, but for QTOF instruments using variable width windowing as well, showing that our observations are generalizable across instrumentation and DIA isolation schemes. As DIA methods can acquire both MS1 and MS2 measurements, we are able to compare the quantification of SILAC based on precursor or fragment ions. Theoretically, we should expect that MS2-based quantification (whether by DIA or SRM/MRM or PRM) to result in more specific, more sensitive quantification compared to MS1-based quantification (whether full-scans are acquired in conjunction with DIA or PRM MS2 scans) because the fragment-level ions are more specific to a given precursor than the parent ion alone. Additionally, MS2 spectra are, overall, less complex than MS1-level spectra, although the degree of MS2 complexity increases with increasing DIA window width. In part due to the increased specificity of MS2 spectra, fragment-level quantification tends to suffer from less interference as well. That said, recent work has shown that combining MS1- and MS2-level information into one quantification gives improvements over either alone (Huang et al., 2020), but is regrettably proprietary and therefore we were not able to explore combining MS1- and MS2-level information in this work. Regardless, it is clear that MS2-based quantification of SILAC samples outperforms MS1-level quantification in both accuracy and reproducibility, which is particularly pronounced at extreme SILAC ratios.

Finally, the quantitative benefits of DIA for pulseSILAC give rise to more reproducible half-life estimates. Between technical replicates, where the same half-life value is expected, DIA gives more precise turnover models and therefore more reproducible half-life estimates. We expect that more sophisticated turnover models that take advantage of DIA data assumptions, such as left-censored missingness and heteroskedasticity, would further benefit the accuracy and precision of half-life estimation and therefore the study of differentially

Author Manuscript Author Manuscript Author Manuscript Author Manuscript

degradation of proteins. Therefore, while SILAC-DIA could potentially be used for multiplex experiments, where a light and heavy sample are combined at an equimolar ratio (duplexing), it is our recommendation that the best application for SILAC-DIA is pSILAC turnover experiments, where more precise and accurate quantification at extreme ratios can be used to fit more sensitive turnover models.

As our approach for processing pSILAC-DIA described here is readily performed with freely available open-source software and is detailed with a full tutorial (Supplementary Note 1), and with the sustained interest in using DIA approaches, we anticipate this workflow becoming a popular choice for pulse SILAC-based protein turnover experiments.

Supplementary Material

Refer to Web version on PubMed Central for supplementary material.

ACKNOWLEDGEMENTS

This work was supported by the National Institutes of Health R01GM110174 and P01AG031862 and by Celgene to BAG; and by the National Institutes of Health/National Cancer Institute T32CA009140 to LKP. B.S. was supported by a Nathan Shock Center Pilot Award (University of Washington). Computational resources were supported by NIH Project Grant S10OD023592. We additionally acknowledge the support of instrumentation from the NCRR shared instrumentation grant 1S10 OD016281 to the Buck Institute.

REFERENCES

1. Bantscheff M, Schirle M, Sweetman G, Rick J & Kuster B Quantitative mass spectrometry in proteomics: a critical review. Anal. Bioanal. Chem 389, 1017–1031 (2007). [PubMed: 17668192]
2. Pino LK, Rose J, O'Broin A, Shah S & Schilling B Emerging mass spectrometry-based proteomics methodologies for novel biomedical applications. Biochem. Soc. Trans BST20191091 (2020) doi:10.1042/BST20191091.
3. Ong S-E, Kratchmarova I & Mann M Properties of ^{13}C-Substituted Arginine in Stable Isotope Labeling by Amino Acids in Cell Culture (SILAC). J. Proteome Res 2, 173–181 (2003). [PubMed: 12716131]
4. Gillet LC et al. Targeted Data Extraction of the MS/MS Spectra Generated by Data-independent Acquisition: A New Concept for Consistent and Accurate Proteome Analysis. Mol. Cell. Proteomics 11, O111.016717 (2012).
5. Collins BC et al. Multi-laboratory assessment of reproducibility, qualitative and quantitative performance of SWATH-mass spectrometry. Nat. Commun 8, (2017).
6. Minogue CE et al. Multiplexed Quantification for Data-Independent Acquisition. Anal. Chem 87, 2570–2575 (2015). [PubMed: 25621425]
7. Di Y, Zhang Y, Zhang L, Tao T & Lu H MdFDIA: A Mass Defect Based Four-Plex Data-Independent Acquisition Strategy for Proteome Quantification. Anal. Chem 89, 10248–10255 (2017). [PubMed: 28872844]
8. Klann K & Münch C Instrument Logic Increases Identifications during Mutliplexed Translatome Measurements. Anal. Chem 92, 8041–8045 (2020). [PubMed: 32442378]
9. Ludwig C et al. Data-independent acquisition-based SWATH-MS for quantitative proteomics: a tutorial. Mol. Syst. Biol 14, e8126 (2018). [PubMed: 30104418]
10. Luo Y et al. SWATH-based proteomics identified carbonic anhydrase 2 as a potential diagnosis biomarker for nasopharyngeal carcinoma. Sci. Rep 7, 41191 (2017). [PubMed: 28117408]
11. Bruderer R et al. Extending the Limits of Quantitative Proteome Profiling with Data-Independent Acquisition and Application to Acetaminophen-Treated Three-Dimensional Liver Microtissues. Mol. Cell. Proteomics 14, 1400–1410 (2015). [PubMed: 25724911]

Author Manuscript Author Manuscript Author Manuscript Author Manuscript

12. Haynes SE, Majmudar JD & Martin BR DIA-SIFT: A Precursor and Product Ion Filter for Accurate Stable Isotope Data-Independent Acquisition Proteomics. Anal. Chem 90, 8722–8726 (2018). [PubMed: 29989796]
13. Tackett AJ et al. I-DIRT, A General Method for Distinguishing between Specific and Nonspecific Protein Interactions. J. Proteome Res 4, 1752–1756 (2005). [PubMed: 16212429]
14. Boisvert F-M et al. A Quantitative Spatial Proteomics Analysis of Proteome Turnover in Human Cells. Mol. Cell. Proteomics 11, M111.011429 (2012).
15. Schwanhäusser B, Gossen M, Dittmar G & Selbach M Global analysis of cellular protein translation by pulsed SILAC. PROTEOMICS 9, 205–209 (2009). [PubMed: 19053139]
16. Doherty MK, Hammond DE, Clague MJ, Gaskell SJ & Beynon RJ Turnover of the Human Proteome: Determination of Protein Intracellular Stability by Dynamic SILAC. J. Proteome Res 8, 104–112 (2009). [PubMed: 18954100]
17. Kristensen LP et al. Temporal Profiling and Pulsed SILAC Labeling Identify Novel Secreted Proteins During *Ex Vivo* Osteoblast Differentiation of Human Stromal Stem Cells. Mol. Cell. Proteomics 11, 989–1007 (2012). [PubMed: 22801418]
18. Pozniak Y et al. System-wide Clinical Proteomics of Breast Cancer Reveals Global Remodeling of Tissue Homeostasis. Cell Syst. 2, 172–184 (2016). [PubMed: 27135363]
19. Dai D-F et al. Altered proteome turnover and remodeling by short-term caloric restriction or rapamycin rejuvenate the aging heart. Aging Cell 13, 529–539 (2014). [PubMed: 24612461]
20. Huo Y et al. Stable isotope-labelling analysis of the impact of inhibition of the mammalian target of rapamycin on protein synthesis. Biochem. J 444, 141–151 (2012). [PubMed: 22428559]
21. Savitski MM et al. Multiplexed Proteome Dynamics Profiling Reveals Mechanisms Controlling Protein Homeostasis. Cell 173, 260–274.e25 (2018). [PubMed: 29551266]
22. Basisty N, Holtz A & Schilling B Accumulation of “Old Proteins” and the Critical Need for MS-based Protein Turnover Measurements in Aging and Longevity. PROTEOMICS 20, 1800403 (2020).
23. Keshishian H, Addona T, Burgess M, Kuhn E & Carr SA Quantitative, Multiplexed Assays for Low Abundance Proteins in Plasma by Targeted Mass Spectrometry and Stable Isotope Dilution. Mol. Cell. Proteomics 6, 2212–2229 (2007). [PubMed: 17939991]
24. Searle BC et al. Chromatogram libraries improve peptide detection and quantification by data independent acquisition mass spectrometry. Nat. Commun 9, (2018).
25. Amodei D et al. Improving Precursor Selectivity in Data-Independent Acquisition Using Overlapping Windows. J. Am. Soc. Mass Spectrom 30, 669–684 (2019). [PubMed: 30671891]
26. Pino LK, Just SC, MacCoss MJ & Searle BC Acquiring and Analyzing Data Independent Acquisition Proteomics Experiments without Spectrum Libraries. Mol. Cell. Proteomics mcp.P119.001913 (2020) doi:10.1074/mcp.P119.001913.
27. Schilling B, Gibson BW & Hunter CL Generation of High-Quality SWATH® Acquisition Data for Label-free Quantitative Proteomics Studies Using TripleTOF® Mass Spectrometers. in Proteomics (eds. Comai L, Katz JE & Mallick P) vol. 1550 223–233 (Springer New York, 2017).
28. Chambers MC et al. A cross-platform toolkit for mass spectrometry and proteomics. Nat. Biotechnol 30, 918–920 (2012). [PubMed: 23051804]
29. Gessulat S et al. Prosit: proteome-wide prediction of peptide tandem mass spectra by deep learning. Nat. Methods 16, 509–518 (2019). [PubMed: 31133760]
30. Searle BC et al. Generating high quality libraries for DIA MS with empirically corrected peptide predictions. Nat. Commun 11, 1548 (2020). [PubMed: 32214105]
31. Solntsev SK, Shortreed MR, Frey BL & Smith LM Enhanced Global Post-translational Modification Discovery with MetaMorpheus. J. Proteome Res 17, 1844–1851 (2018). [PubMed: 29578715]
32. Vizcaíno JA et al. ProteomeXchange provides globally coordinated proteomics data submission and dissemination. Nat. Biotechnol 32, 223–226 (2014). [PubMed: 24727771]
33. Sharma V et al. Panorama: A Targeted Proteomics Knowledge Base. J. Proteome Res 13, 4205–4210 (2014). [PubMed: 25102069]

Author Manuscript Author Manuscript Author Manuscript Author Manuscript

34. Welle KA et al. Time-resolved Analysis of Proteome Dynamics by Tandem Mass Tags and Stable Isotope Labeling in Cell Culture (TMT-SILAC) Hyperplexing. Mol. Cell. Proteomics 15, 3551–3563 (2016). [PubMed: 27765818]

35. Navarro P et al. A multicenter study benchmarks software tools for label-free proteome quantification. Nat. Biotechnol 34, 1130–1136 (2016). [PubMed: 27701404]

36. Moumen A, Masterson P, O'Connor MJ & Jackson SP hnRNP K: An HDM2 Target and Transcriptional Coactivator of p53 in Response to DNA Damage. Cell 123, 1065–1078 (2005). [PubMed: 16360036]

37. Baugh JM & Pilipenko EV 20S Proteasome Differentially Alters Translation of Different mRNAs via the Cleavage of eIF4F and eIF3. Mol. Cell 16, 575–586 (2004). [PubMed: 15546617]

38. Garcia M et al. Biological and Clinical Significance of Cathepsin D in Breast Cancer Metastasis. Stem Cells 14, 642–650 (1996). [PubMed: 8948022]

Author Manuscript Author Manuscript Author Manuscript Author Manuscript

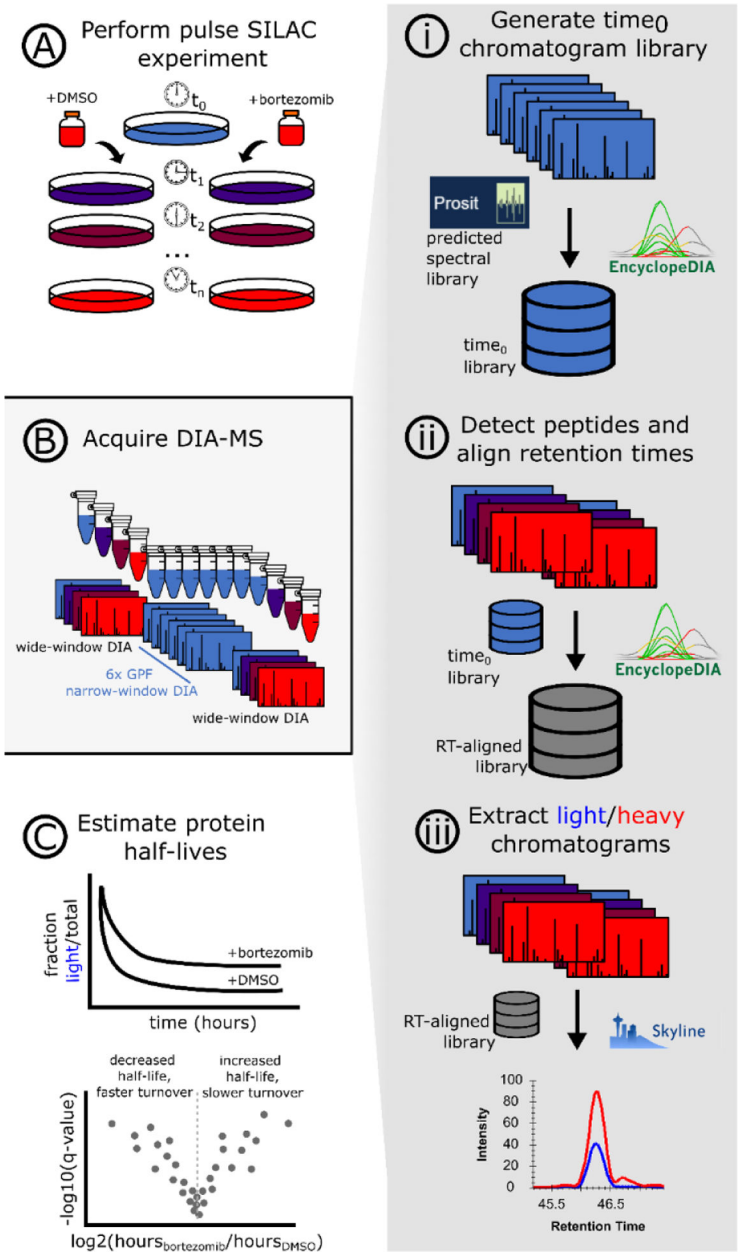

Figure 1. An approach for quantifying pulse SILAC peptides using free, open-source software.

A pulse SILAC experiment is performed **(A)** and the data is acquired following a chromatogram library approach **(B)** in which the time$_0$ sample(s) are injected multiple times with gas phase fractionation (GPF). The GPF time$_0$ spectra files are searched against a predicted spectral library using EncyclopeDIA, creating a time$_0$ chromatogram library **(i)** which is then used to align the light peptide retention times across the entire pulse SILAC experiment **(ii)**. Using the database of retention time-aligned light peptide detections, the heavy peptides are paired and chromatograms extracted using Skyline **(iii)**. Quantitative values for light and heavy SILAC peptides are used to fit protein turnover models and assess statistical significance **(C)**.

Author Manuscript Author Manuscript Author Manuscript Author Manuscript

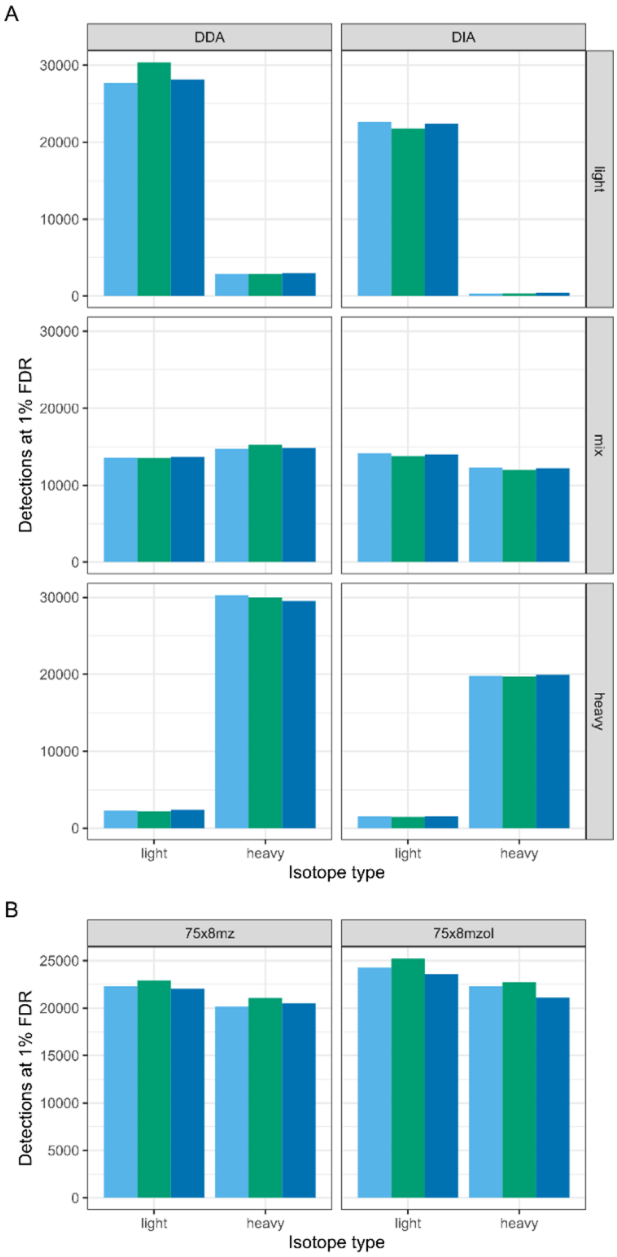

Figure 2. Comparison of PSM and peptide detections in SILAC-DDA vs SILAC-DIA.

(A) Detections in three SILAC proteome samples (100% light SILAC, 100% heavy SILAC, and 50/50% light/heavy SILAC "mix") are compared from three replicates each of DDA and DIA (windowing scheme of 75×8 m/z, staggered). For DDA analysis, the unique PSMs at 1% FDR are used, without using match-between-runs across samples; for DIA analysis, the unique peptides at 1% FDR are used. (B) The number of unique peptides detected at 1% FDR in each technical triplicate of two DIA windowing schemes is compared for the same 50/50% light/heavy SILAC sample. Schemes are described by the number of isolation windows (e.g. "75") followed by the width of the isolation windows (e.g. "x8mz"), and whether the isolation windows are staggered ("stagger") or fixed.

Author Manuscript Author Manuscript Author Manuscript Author Manuscript

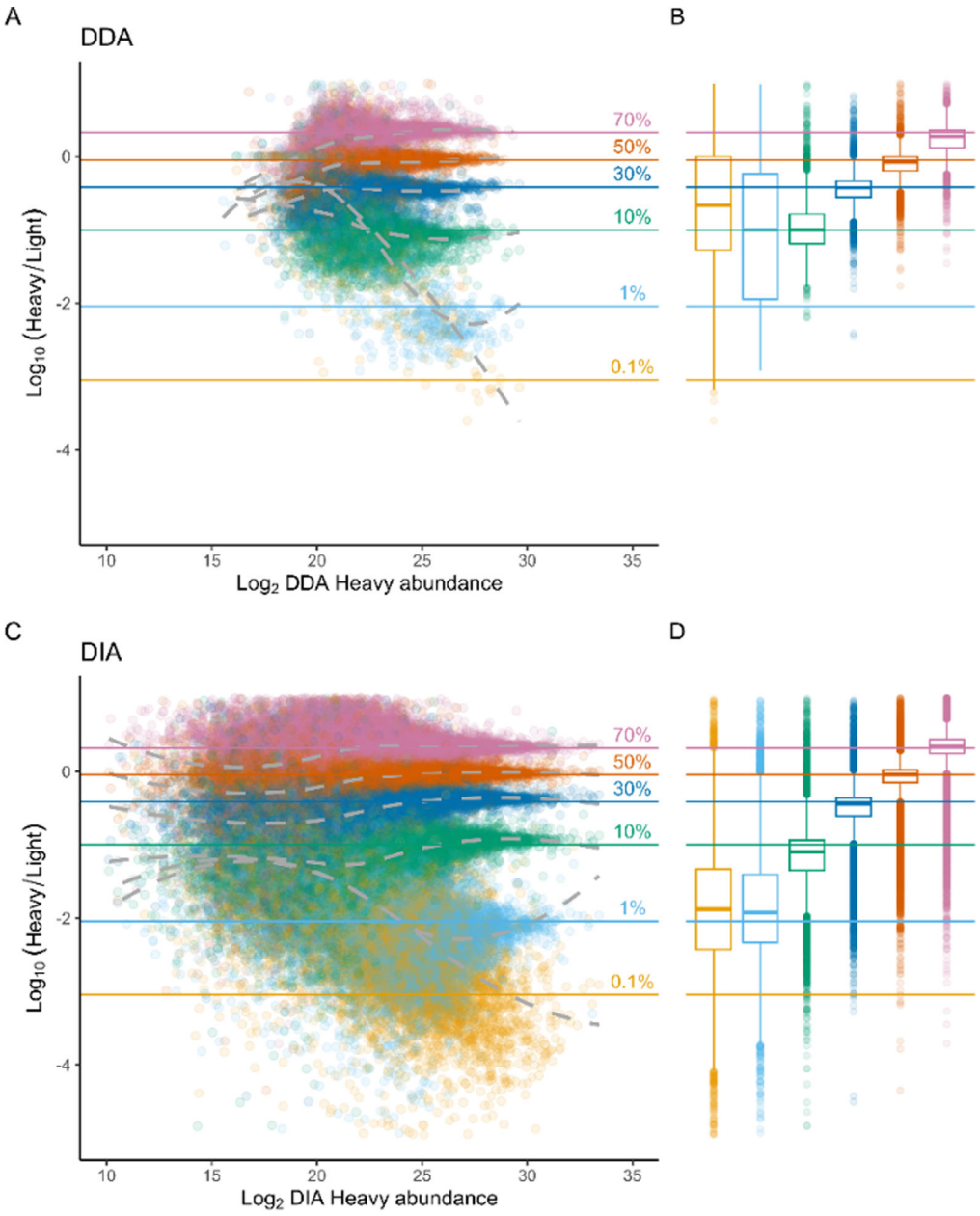

Fig 3. SILAC-DIA improves dynamic range and quantitative accuracy in benchmark experiments.

The measured log10(heavy/light) ratios in four dilutions of heavy/light HeLa proteome samples are compared using DDA MS1 quantification with match-between-runs (A, B) enabled versus DIA MS2 quantification (C, D). The samples represent a 70%/30% heavy/light proteome (pink, “0.7”), 50%/50% (orange, “0.5”), 30%/70% (blue, “0.5”), 10/90% (green, “0.1”), 1%/99% (cyan, “0.01”), and a 0.1%/99.9% (yellow, “0.001”). Boxplots depict the first and third quartiles (25th and 75th percentiles) of the Log10(Heavy/Light) values for each sample, with whiskers representing 1.5x the interquartile range.

Author Manuscript Author Manuscript Author Manuscript Author Manuscript

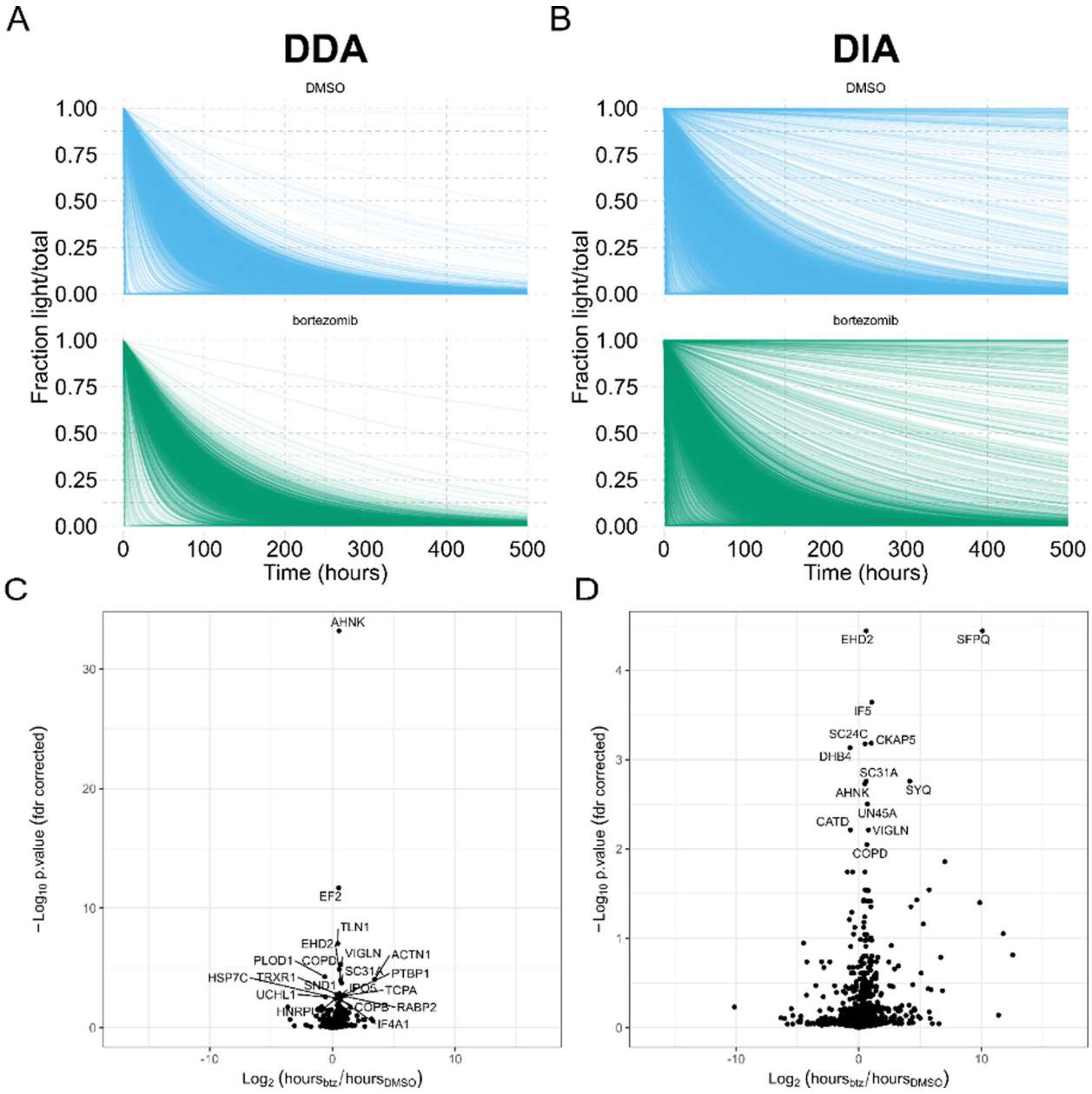

Figure 4. Protein turnover for bortezomib treated cell cultures.

(A, B) Time is shown horizontally with the fraction of light/total protein vertically. DMSO treatment is shown in blue and bortezomib treatment in green. The shape of these models indicates degradation rate, where proteins with sharply decreasing light fractions are being rapidly degraded, while proteins with more gradual decreases in light fraction are more slowly degraded. **(C, D)** Volcano plots of significantly differential protein half-lives are shown for DDA and DIA analyses of the same samples for DDA (left) and DIA (right).

Author Manuscript Author Manuscript Author Manuscript Author Manuscript

Table 1.

Significantly differentially degraded proteins (bortezomib vs DMSO) found by both DDA and DIA half-life estimation.

The twelve shared proteins found to be differential using both the DDA and the DIA datasets are shown along with the log2 fold change (bortezomib/DMSO) calculated by each dataset.

Uniprot Accession	Gene Name	Change in protein half-life (hours) DDA	Change in protein half-life (hours) DIA	Description
P51659	DHB4	−20.9	−30.15	Peroxisomal multifunctional enzyme type 2 (MFE-2)
P07339	CATD	−22.5	−19.1	Cathepsin D precursor
O15460	P4HA2	−21.9	−30.1	Prolyl 4-hydroxylase subunit alpha-2 (4-PH alpha-2)
P61978	HNRPK	13.6	12.3	Heterogeneous nuclear ribonucleoprotein K (hnRNP K) (Transformation up-regulated nuclear protein) (TUNP)
Q09666	AHNK	18.4	17.7	Neuroblast differentiation-associated protein AHNAK (Desmoyokin)
Q9NZN4	EHD2	16.6	18.1	EH domain-containing protein 2 (PAST homolog 2)
P48444	COPD	18.2	18.1	Coatomer subunit delta (Archain) (Delta-coat protein) (Delta-COP)
Q14152	EIF3A	20.2	13.7	Eukaryotic translation initiation factor 3 subunit A (eIF3a)
P60842	IF4A1	22.7	20.0	Eukaryotic initiation factor 4A-I (eIF-4A-I)
Q00341	VIGLN	17.9	21.9	Vigilin (High density lipoprotein-binding protein) (HDL-binding protein)
O94979	SC31A	22.4	18.2	Protein transport protein Sec31A (ABP125) (ABP130)
Q16222	UAP1	22.6	20.6	UDP-N-acetylhexosamine pyrophosphorylase (Antigen X) (AGX)